Polym. Bull. (2011) 67:1201–1213
DOI 10.1007/s00289-011-0449-4

ORIGINAL PAPER

Preparation and evaluation of *O*-carboxymethyl chitosan/cyclodextrin nanoparticles as hydrophobic drug delivery carriers

Jingou Ji · Shilei Hao · Weiqi Liu · Jingfen Zhang · Danjun Wu · Yi Xu

Received: 23 September 2010 / Revised: 7 December 2010 / Accepted: 6 January 2011 /
Published online: 20 January 2011
© Springer-Verlag 2011

Abstract In present study, novel composite nanocarriers comprised of *O*-carboxymethyl chitosan/*β*-cyclodextrin (*O*-CMC/*β*-CD) nanoparticles (NPS) were prepared and used to improve the bioavailability of hydrophobic drugs. Ibuprofen (IBU) was selected as a model drug and chitosan/*β*-CD (CS/*β*-CD) NPS were also prepared as control. The prepared NPS were characterized by FT-IR spectroscopy and X-ray diffraction. IBU entrapment of up to 93.25 ± 2.89% was obtained as determined by UV spectrophotometer. The NPS were spherical in shape with average particle sizes of 166 nm. The in vitro release studies were performed in simulated gastric medium (pH 1.2) and simulated intestinal medium (pH 6.8). The release rate of IBU from the *O*-CMC/*β*-CD NPS was slower than CS/*β*-CD NPS in simulated gastric medium. However, the converse tendency was observed in simulated intestinal medium. These results suggested that *O*-CMC/*β*-CD NPS were more suitable for the oral delivery of hydrophobic drugs compared with the CS/*β*-CD NPS.

Keywords Chitosan · *O*-Carboxymethyl · Cyclodextrin · Ibuprofen · Bioavailability

Introduction

The key biopharmaceutical characteristics impacting the bioavailability and the likelihood of obtaining a good in vitro/in vivo correlation are the drug solubility and

J. Ji (✉) · S. Hao · W. Liu · J. Zhang · D. Wu · Y. Xu
Faculty of Pharmacy, College of Chemistry and Chemical Engineering,
University of Chongqing, Chongqing 400030, China
e-mail: jingou_ji@yahoo.com.cn

permeability [1]. In most cases, hydrophobic compounds are prepared in amorphous form, grinding, solid dispersion, and micelle to improve their aqueous solubility [2]. Actually, cyclodextrins (CDs) such as β-cyclodextrin (β-CD) are also used to improve the solubility, stability, and bioavailability of hydrophobic drugs. β-CD has a lipophilic inner cavity and hydrophilic outer surfaces; it can facilitate the inclusion of a large variety of guest molecules stabilized by a series of weak intermolecular forces.

In recent years, chitosan (CS) nanoparticles (NPS) have become important carriers in drug delivery because of the favorable features of the polymer in terms of biocompatibility, biodegradability, and nontoxic properties [3–8]. CS NPS can improve the bioavailability of drug by improving the absorption of drugs in vivo and enhancing the intracellular penetration [9]. Due to the nature of the polymer, it is difficult to entrap hydrophobic drugs into CS NPS. Therefore, CS/CD NPS with the advantages of good solubilization and permeability would increase the loading capacity and improve the bioavailability of hydrophobic drugs [10–12].

However, the major drawback of CS is insolubility in pure water for its application in drug delivery systems [13]. *O*-Carboxymethyl chitosan (*O*-CMC), an amphiprotic polymer containing carboxyl (COOH) and amine (NH_2) groups, is a kind of water-soluble CS derivative [14]. It can synthesize NPS with calcium chloride ($CaCl_2$) via cross-linking in neutral or weakly basic conditions. Furthermore, *O*-CMC also has good properties such as low toxicity, good biocompatibility, biodegradability, controlling the drug release and delivery the drug to a target site [15–17].

Ibuprofen (IBU, 2-methyl-4-(2-methylpropyl) phenylacetic acid) is a non-steroidal anti-inflammatory drug (NSAID) used for the treatment of inflammatory, pyretic, and mild analgesic diseases [18]. The bioavailability of the drug after oral administration is low because of its poor water solubility and short plasma half-life of 1–3 h [19]. The aim of the present study was to synthesize a novel *O*-CMC/β-CD NPS as the IBU delivery carrier. The preparation, characterization, and in vitro release behavior of the NPS is described.

Experimental

Materials

Chitosan (CS, deacetylation degree 95%, molecular weight 80 kDa) was purchased from Golden-shell Biochemical Co. Ltd. (Zhejiang, China). *O*-Carboxymethyl chitosan (*O*-CMC, 90% *O*-carboxymethyl groups per repeating unit) was purchased from Qingdao Honghai Bio-tech Co. Ltd. (Shandong, China). Tripolyphosphate (TPP) was purchased from Dongsheng Chemical reagent Co. Ltd. (Zhejiang, China). Ibuprofen (IBU) was kindly gifted by Southwest Pharmaceutical Co. Ltd. (Chongqing, China). β-Cyclodextrin (β-CD) was purchased from Kelong Chemical reagent Co. Ltd. (Sichuan, China). All other materials and reagents used in the study were analytical grade.

Phase solubility studies

Phase solubility studies were performed according to the method described by Higuchi and Conners [20]. In brief, an overdose of IBU (50 mg) was added to 20 mL pure water containing various amount of β-CD (from 0 to 6 mmol) in the presence or absence of a fix amount of *O*-CMC (0.2%, w/v). Then the solutions were shaken at 30 °C for 48 h. After equilibrium, the aliquots were filtered through 0.45 μm cellulose acetate membrane filters (New Asiatic Pharmaceutical, China). The filtrates were diluted and assayed by the UV spectrophotometer (Shimadzu, UV-2450, Japan) at 265 nm. Each sample was measured in triplicate. The phase solubility studies of IBU in the presence of CS (0.2%, w/v) were also carried out as control. The phase solubility diagram was plotted as the β-CD concentration versus IBU concentration.

The stability constants, K_c, were calculated as follows from the slope of straight-line portion of the phase solubility diagram, where intercept is the solubility of IBU in the absence of β-CD according to Higuchi–Connors Eq. 1:

$$K_c = \frac{\text{Slope}}{\text{Intercept } (1 - \text{Slope})} \tag{1}$$

Preparation of *O*-CMC/β-CD and CS/β-CD NPS

The *O*-CMC/β-CD NPS were prepared by cross-linking. In brief, *O*-CMC solution (0.2%, w/v) was prepared by dissolving *O*-CMC in pure water at room temperature under sonication. Then IBU and β-CD were added to the *O*-CMC solution, the mixture solution was stirred under the magnetic stirring for 24 h. $CaCl_2$ solution (0.4%, w/v) was added dropwise into the mixture with the mass ratios of *O*-CMC to $CaCl_2$ at 4:1 and 5:1. The composite NPS started to form spontaneously via the $CaCl_2$ initiated ionic cross-linking mechanism. And the NPS suspensions were continuously stirred for 1 h and then centrifuged at 16,000 rpm for 30 min. The resulting NPS were lyophilized and stored.

The preparation of the CS/β-CD NPS was similar to that for the *O*-CMC/β-CD NPS. Acetic acid solution (0.1%, w/v) instead of pure water was used for dissolving CS. TPP solution (0.2%, w/v) was selected as the cross-linking agent. The NPS were prepared selecting the mass ratios of CS to TPP at 6:1 and 7:1.

Characterization of the NPS

The particle size, zeta potential, and polydispersity index (PDI) of the NPS obtained from "Preparation of O-CMC/β-CD and CS/β-CD NPS" section were measured by photon correlation spectroscopy using a nano ZS90 Zetasizer (Malvern Instruments, UK). The samples were prepared with deionized water at appropriate concentrations. The surface morphology of the drug-loaded *O*-CMC/β-CD NPS was observed by SEM. The nanoparticle suspension was spread on a glass plate and dried at room temperature. The dried NPS were coated with gold under vacuum and then examined (Hitachi, S-3400N, Japan).

The chemical structure and complex formation of IBU, β-CD, *O*-CMC, drug-loaded *O*-CMC/β-CD NPS, CS, and drug-loaded CS/β-CD NPS were analyzed by FT-IR (Nicolet, 5DX/550II, USA). The samples were prepared by grinding the dry specimens with KBr and pressing the mixed powder to form disks.

The crystal phase constituent analysis was carried out by X-ray diffractometry (XRD) (Shimadzu, XRD6000X, Japan). IBU, β-CD, *O*-CMC, drug-loaded *O*-CMC/β-CD NPS, CS, and drug-loaded CS/β-CD NPS were scanned from 5° to 40°.

Evaluation of drug loading capacity

The encapsulation efficiency (EE) and the loading efficiency (LE) of the IBU-loaded NPS were determined by following method: the free IBU was separated from the nanoparticle suspensions by centrifugation at 16,000 rpm for 30 min. The amount of free IBU remaining in the supernatant was measured by UV spectrophotometer at 265 nm. A blank sample was made from NPS without loaded IBU but treated similarly as the IBU-loaded NPS. Each sample was measured in triplicate. The EE and LE were calculated by following Eqs. 2 and 3:

$$\mathrm{EE} = \frac{\text{Total amount of IBU} - \text{Free IBU}}{\text{Total amount of IBU}} \tag{2}$$

$$\mathrm{LE} = \frac{\text{Total amount of IBU} - \text{Free IBU}}{\text{Amount of nanoparticles}} \tag{3}$$

In vitro release studies

In vitro release profiles of IBU from drug-loaded *O*-CMC/β-CD and CS/β-CD NPS were carried out for 3 h in simulated gastric (pH 1.2) and intestinal (pH 6.8) medium without enzymes. 20 mg IBU-loaded *O*-CMC/β-CD NPS or CS/β-CD NPS and 5 mL release medium were put into a dialysis tube (MWCO: 12,000). The dialysis tube was placed in 30 mL release medium at 37 °C and stirred continuously at 100 rpm. At specific time intervals, 5 mL were withdrawn and replaced with fresh release medium (5 mL). The concentration of the released IBU was determined by UV spectrophotometer. The analysis was performed in triplicate for each sample.

Results and discussion

Phase solubility studies

The phase solubility profiles for the complex formation between IBU and β-CD are presented in Fig. 1. The diagram shows that the aqueous solubility of the drug increased linearly as a function of β-CD concentration. It is clear that this solubility diagram can be classified as the A_L type according to Higuchi and Connors, indicating the formation of the IBU:β-CD (1:1) inclusion complex [21]. The stability constant (K_c) of IBU:β-CD complex (1:1) in the absence of CS and *O*-CMC

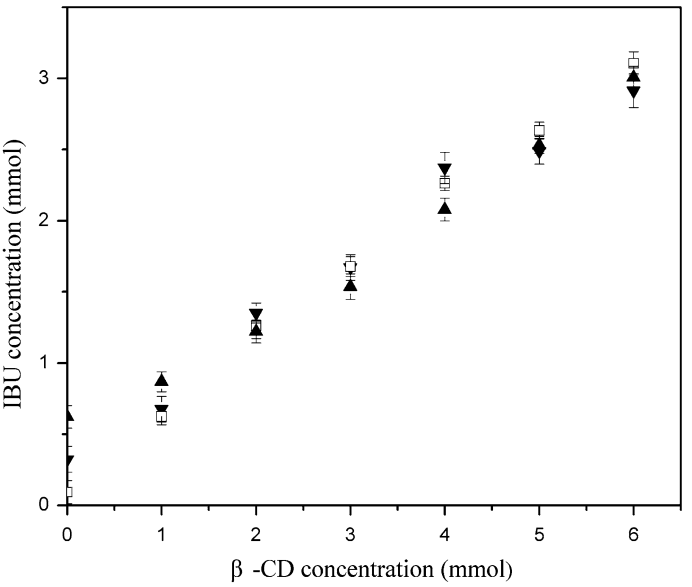

Fig. 1 Phase solubility diagram for IBU and β-CD in water (*inverted triangle*), CS (*square*), and *O*-CMC (*upright triangle*) ($n = 3$)

calculated to be 2.2×10^3 M^{-1} according to the Eq. 1. The K_c of formation in the presence of CS and *O*-CMC was 4.2×10^3 and 1.4×10^3 M^{-1}, respectively. The values were in the range of stability constant value (200–5,000 M^{-1}) [22].

The apparent solubility of IBU in the CS solution was 36 ± 2.3 μg/mL (without β-CD); this was mainly due to the poor solubility of IBU in the acid solution. And the apparent solubility of IBU in the *O*-CMC was $(1.3 \pm 0.1) \times 10^2$ μg/mL. The molar ratio of IBU to β-CD was 1:2 in the diagram, it was indicated that 1 mol IBU could be dissolved in the 2 mol β-CD solution in the absence of any other solubilizing agents, i.e., ethanol, acetone, etc.

Preparation of the CS/CD NPS

The *O*-CMC/β-CD NPS and the CS/β-CD NPS were prepared via the cross-linking method. The feed amount of IBU was determined by the phase solubility studies. In order to limit the usage of organic solvents, the feeding molar ratio of β-CD to IBU was selected as 2:1. The feeding concentration of IBU was selected as 30 and 100 μg/mL in the preparation of the *O*-CMC and CS NPS (without β-CD) according to the phase solubility studies.

The effects of the different mass ratios of *O*-CMC/β-CD/$CaCl_2$ and CS/β-CD/TPP on the loading capacity of NPS are shown in Tables 1 and 2. In Table 1, the mass ratio of *O*-CMC to $CaCl_2$ was selected as 4:1 and 5:1. The NPS without composite β-CD had a low EE and LE. The EE and LE of the NPS with the mass ratio of *O*-CMC to $CaCl_2$ 4:1 were higher than the NPS with the mass ratio 5:1, this trend could be explained that more cross-linking agent could improve the loading

Table 1 Effect of the different mass ratio of *O*-CMC/*β*-CD on the loading capacity of the NPS (mean ± S.D., $n = 3$)

Mass ratio (*O*-CMC/*β*-CD/$CaCl_2$)	EE (%)	LE (%)
4/0/1	51.13 ± 2.58	19.17 ± 1.28
4/0/0.8	44.43 ± 2.64	16.66 ± 2.54
4/2.5/1	79.49 ± 3.81	26.94 ± 3.02
4/2.5/0.8	73.58 ± 4.21	24.27 ± 2.30
4/3/1	75.98 ± 1.62	31.00 ± 1.58
4/3/0.8	72.28 ± 3.22	29.49 ± 2.71

Table 2 Effect of the different mass ratio of CS/*β*-CD on the loading capacity of the NPS (mean ± S.D., $n = 3$)

Mass ratio (CS/*β*-CD/TPP)	EE (%)	LE (%)
6/0/1	45.10 ± 2.05	8.12 ± 1.56
6/0/0.86	26.48 ± 1.45	4.77 ± 3.54
6/1.5/1	95.39 ± 2.15	21.13 ± 2.89
6/1.5/0.86	86.65 ± 3.01	18.06 ± 3.13
6/3/1	93.25 ± 2.89	32.42 ± 2.54
6/3/0.86	85.53 ± 1.24	29.07 ± 1.98

capacity of the NPS. And the EE and LE of the *O*-CMC/*β*-CD NPS were higher than *O*-CMC NPS. The EE of the *O*-CMC/*β*-CD NPS decreased with increasing the amount of *β*-CD and IBU, but the LE of the NPS increased.

In Table 2, the mass ratio of the CS/*β*-CD was selected as 6:1 and 7:1. It was a similar trend with the *O*-CMC/*β*-CD NPS. But the EE and LE of the *O*-CMC NPS were higher than CS NPS (without *β*-CD), which may be related to the higher solubility of IBU in the weakly alkaline *O*-CMC solution than in the acidic CS solution. The LE of CS/*β*-CD NPS ranged from 21.13 ± 2.89 to 32.42 ± 2.54%, which was similar with the *O*-CMC/*β*-CD NPS.

Characterizations of the NPS

Particle size distributions of the IBU-loaded CS/*β*-CD NPS (Fig. 2a) and IBU-loaded *O*-CMC/*β*-CD NPS (Fig. 2b) are shown in Fig. 2. The average size of the IBU-loaded *O*-CMC/*β*-CD NPS was 166 nm and the PDI was 0.164, exhibiting relatively narrow particle size distributions. The average size of the CS/*β*-CD NPS was 199 nm and the PDI was 0.197. The zeta potential of the *O*-CMC/*β*-CD NPS and the CS/*β*-CD NPS were −23.65 and +37.19 mV, respectively.

The morphological characteristics of the IBU-loaded *O*-CMC/*β*-CD NPS were examined using the SEM and the results are shown in Fig. 3. The results suggested that the IBU-loaded NPS were spherical in shape and the average size was about 200 nm.

Figure 4 depicts the FT-IR spectra of *β*-CD, IBU, IBU-loaded CS/*β*-CD NPS, CS, IBU-loaded *O*-CMC/*β*-CD NPS, and *O*-CMC. The characteristic peaks of *β*-CD including at 3400 cm^{-1} (–OH stretching), 2927 cm^{-1} (–CH stretching), 1400 cm^{-1}

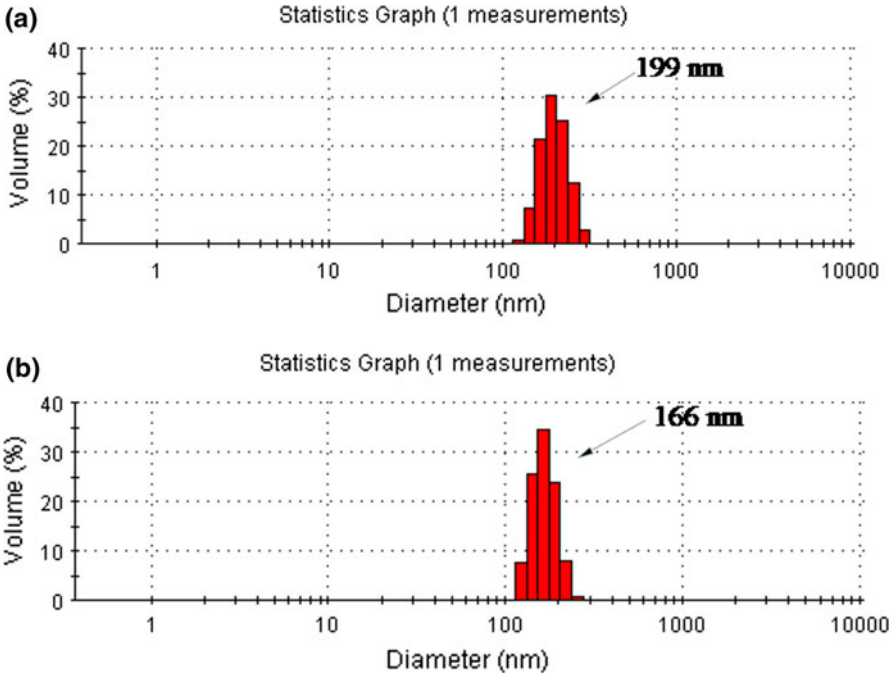

Fig. 2 Particles size distribution the IBU-loaded CS/β-CD NPS (**a**) and IBU-loaded *O*-CMC/β-CD NPS (**b**)

(–OH bending), and 950 cm^{-1} (skeletal vibration involving a 1,4 linkage) [23]. The characteristic peaks of IBU including at 1721 cm^{-1} (–C=O stretching, from a carboxylic acid group), at 1415 cm^{-1} (–C=O stretching, from a ketonic), at 1320 and 1225 cm^{-1} (–OH bending). In the IR spectrum of *O*-CMC, a characteristic peaks at 3431 cm^{-1} (–NH_2 and –OH stretching), at 2926 cm^{-1} (–CH stretching from aliphatic), at 1600 cm^{-1} (–NH bending), at 1408 cm^{-1} (–COO^- stretching), and 1325 cm^{-1} (–C–O stretching). Another strong peak at 1074 cm^{-1} corresponds to the secondary hydroxyl group C–O, indicating that the carboxymethyl substitution occurs at the C_6 position. For *O*-CMC/β-CD NPS, the peak at 3431 cm^{-1} shifts to the lower wave number (3412 cm^{-1}), the peak at 2926 cm^{-1} shows a shift to higher wave number (2949 cm^{-1}). And the peak at 1325 cm^{-1} becomes weaker, which indicates that the cross-linking reaction between carboxyl groups of *O*-CMC and calcium chloride has occurred [24, 25].

The results also demonstrate the basic features of CS at 3426 cm^{-1} (–OH and –NH_2 stretching), 2922 and 2872 cm^{-1} (–CH stretching), 1601 cm^{-1} (–NH_2 stretching), 1078 cm^{-1} (C–O–C stretching). For IBU-loaded CS/β-CD NPS, the peak of 3423 cm^{-1} becomes wider, indicating that hydrogen bonding is enhanced between CS and β-CD. The –NH_2 bending vibration shifts from 1601 to 1542 cm^{-1}, and a new peak appear at 1637 cm^{-1}, which indicates that some interaction between NH_3^+ groups of CS and TPP has occurred within the NPS. The character peak of IBU and β-CD do not appear in the NPS spectra. The results may indicate that there

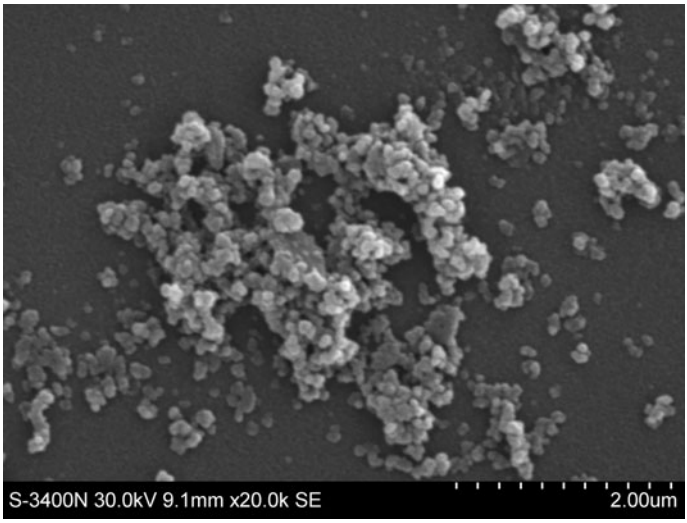

Fig. 3 SEM image of the IBU-loaded *O*-CMC/*β*-*CD* NPS

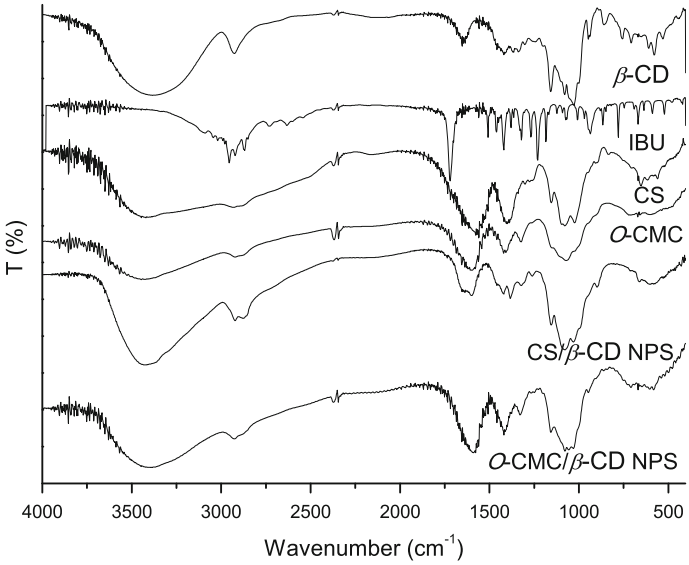

Fig. 4 FT-IR spectra of *β*-CD, IBU, CS, *O*-CMC, IBU-loaded CS/*β*-CD NPS, and IBU-loaded *O*-CMC/*β*-CD NPS

is little surface drug on the NPS and most of drug has been successfully loaded into the NPS.

The XRD patterns of IBU, *β*-CD, IBU-loaded CS/*β*-CD NPS, CS, IBU-loaded *O*-CMC/*β*-CD NPS, and *O*-CMC are illustrated in Fig. 5. IBU and *β*-CD have specific sharp crystal peaks and CS has two specific broad peaks. And the *O*-CMC

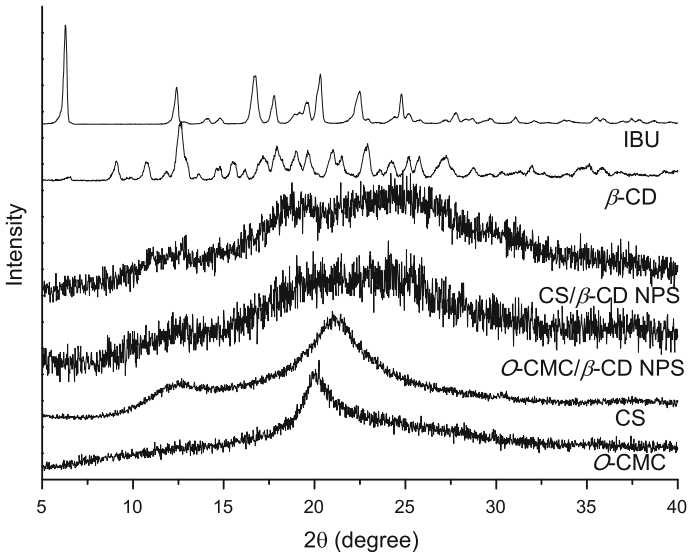

Fig. 5 XRD patterns of IBU, β-CD, IBU-loaded CS/β-CD NPS, IBU-loaded *O*-CMC/β-CD NPS, CS, and *O*-CMC

has a broad peak. When the *O*-CMC/β-CD NPS were synthesized, new peaks at 2θ of 18° and 24° appear and the peak at 2θ 20° becomes even broader and amorphous. Furthermore, after the CS cross-linking with TPP, the basic diffraction peaks are maintained and the peak intensities are decreased. The XRD peak depends on the crystal size, so the peaks of *O*-CMC and CS become broader that may due to the crystalline structure being destroyed and the crystallinity disappearing through the ionic cross-linking effect [26]. The specific sharp crystal peaks of IBU and β-CD are not observed, which may indicate that IBU and β-CD have uniformly dispersed in the NPS in amorphous forms.

In vitro release studies

In vitro release of the *O*-CMC/β-CD NPS and the CS/β-CD NPS was carried out in simulated gastric medium (pH 1.2) and intestinal medium (pH 6.8) for 3 h. And the release profiles of IBU from the two NPS in simulated gastric and intestinal medium are shown in Figs. 6 and 7.

In simulated gastric medium, about 34 and 38% IBU were released from the *O*-CMC/β-CD NPS and the CS/β-CD NPS, respectively, in 3 h. The release rate of CS/β-CD NPS was faster than *O*-CMC/β-CD NPS, the reason could be that both CS and *O*-CMC dissolve in the acidic solution (pH 1.2), and the degradation rate of CS. And the particle size of IBU-loaded CS/β-CD NPS is larger than that of IBU-loaded *O*-CMC/β-CD NPS. Larger size will increase the rate of fluid ingress into the matrix and the degradation rate of CS, which all will increase the release rate of drug from the NPS. NPS in simulated gastric was faster than *O*-CMC NPS. In simulated intestinal medium, these trends were inverted: about 59 and 32% IBU were released

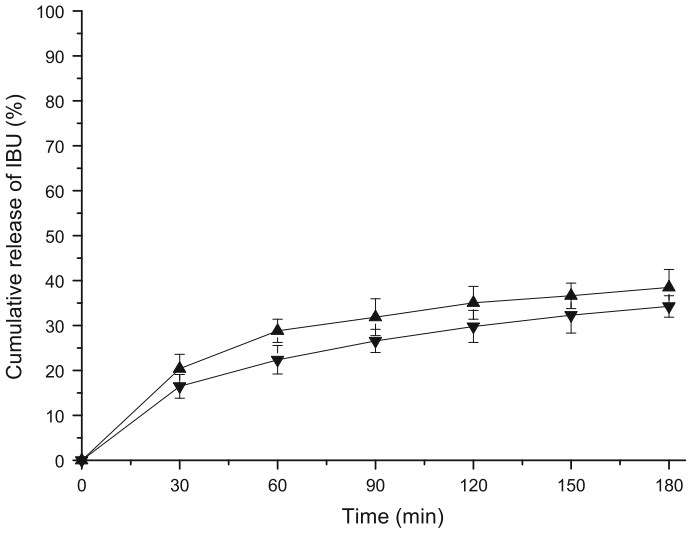

Fig. 6 In vitro release of IBU from CS/β-CD NPS (*upright triangle*) and the *O*-CMC/β-CD NPS (*inverted triangle*) in the simulated gastric medium (pH 1.2) ($n = 3$; CS/β-CD/TPP: 6/3/1; *O*-CMC/β-CD/$CaCl_2$: 4/3/1)

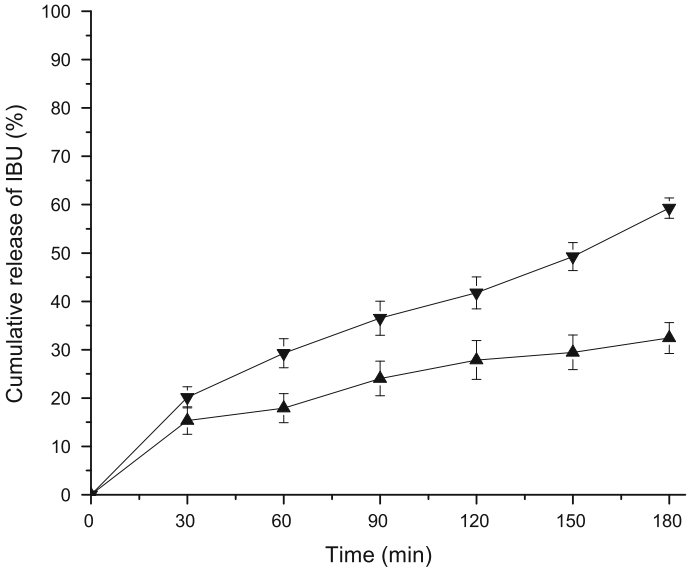

Fig. 7 In vitro release of IBU from CS/β-CD NPS (*upright triangle*) and the *O*-CMC/β-CD NPS (*inverted triangle*) in the simulated intestinal medium (pH 6.8) ($n = 3$; CS/β-CD/TPP: 6/3/1; *O*-CMC/β-CD/$CaCl_2$: 4/3/1)

from the *O*-CMC/β-CD NPS and CS/β-CD NPS in 3 h. This may be due to the fact that *O*-CMC dissolve in the approximately neutral release medium (pH 6.8), but CS was insoluble in the neutral or weakly basic pH range. So the degradation rate of

Table 3 Release kinetic of IBU from the NPS

Release medium	*O*-CMC/*β*-CD NPS			CS/*β*-CD NPS		
	r^2	*n*	*k*	r^2	*n*	*k*
Simulated gastric	0.995	0.464	0.228	0.972	0.347	0.271
Simulated intestinal	0.987	0.579	0.294	0.967	0.440	0.198

O-CMC/*β*-CD NPS in simulated intestinal medium was faster than CS/*β*-CD NPS. The results revealed that *O*-CMC/*β*-CD NPS seem to be more suitable for oral delivery of hydrophobic drug than CS/*β*-CD NPS.

The data of the in vitro release of the IBU from the two NPS in simulated gastric and intestinal medium had been further substantiated by fitting to the Korsmeyer–Peppas model, which was used to determine the mechanism of the initial portion drug release (i.e., $M_t/M_\infty \leq 60\%$), the Eq. 4 as follow [27]:

$$\frac{M_t}{M_\infty} = kt^n \tag{4}$$

In the above equation, *n* represents the diffusional exponent, *k* is kinetic constant, and the correlation coefficient of the model is represented by r^2 value. The values of r^2, *n* and *k* have been calculated and the results obtained are shown in Table 3. The *n* values indicated that the drug release from CS/*β*-CD NPS and *O*-CMC/*β*-CD NPS followed non-Fickian or anomalous diffusion [28]. And the values of *k* suggested that *O*-CMC/*β*-CD NPS were more suitable for the oral delivery of hydrophobic drugs.

Conclusion

In order to improve hydrophobic drug's bioavailability, novel composite NPS of *O*-CMC/*β*-CD were synthesized by a simple ionic cross-linking method. The CS/*β*-CD NPS were also prepared as control. IBU, a hydrophobic drug, was selected as the model compound. The LE of the *O*-CMC/*β*-CD was about 30% with an average size of 166 nm, which were similar with the CS/*β*-CD NPS. It was found that the loading capacity of the *O*-CMC/*β*-CD was higher than *O*-CMC NPS, which indicated that *β*-CD had the strong effect on increasing the solubility of the hydrophobic drug and improving the loading capacity of NPS. The release rate of IBU from *O*-CMC/*β*-CD was slower than CS/*β*-CD NPS in simulated gastric medium, and the inverted trend was observed in simulated intestinal medium, which suggested that the *O*-CMC/*β*-CD NPS seemed to be more suitable for the oral hydrophobic drug delivery.

Acknowledgments This research was supported by Chongqing University Postgraduates' Science and Innovation Fund (201005A1A0010333) and 211 Project Innovation Personnel Training Plan Items of Chongqing University (S-09103).

References

1. Levis KA, Lane ME, Corrigan OI (2003) Effect of buffer media composition on the solubility and effective permeability coefficient of ibuprofen. Int J Pharm 253:49–59
2. Terao K, Nakata D, Fukumi H, Schmid G, Arima H, Hirayama F, Uekama K (2006) Enhancement of oral bioavailability of coenzyme Q_{10} by complexation with γ-cyclodextrin in healthy adults. Nutr Res 26:503–508
3. Chang YH, Xiao L, Du YM (2009) Preparation and properties of a novel thermosensitive *N*-trimethyl chitosan hydrogel. Polym Bull 63:53–545
4. Tang YF, Zhao YY, Li Y, Du YM (2010) A thermosensitive chitosan/poly(vinyl alcohol) hydrogel containing nanoparticles for drug delivery. Polym Bull 64:791–804
5. Lertsutthiwong P, Rojsitthisak P, Nimmannit U (2009) Preparation of turmeric oil-loaded chitosan-alginate biopolymeric nanocapsules. Mater Sci Eng C 29:856–860
6. Du YM, Xia ZY, Lu R (1997) Blend films of chitosan/starch. J Wuhan Univ Nat Sci 2(2):220–224
7. Feng T, Du YM, Li J, Wei YN, Yao PJ (2007) Antioxidant activity of half N-acetylated water-soluble chitosan in vitro. Eur Food Res Technol 225:133–138
8. Chang YH, Xiao L, Du YM (2009) Preparation and properties of a novel thermosensitive N-trimethyl chitosan hydrogel. Polym Bull 63:531–545
9. Soppimath KS, Aminabhavi TM, Kulkarni AR, Rudzinski WE (2001) Biodegradable polymeric nanoparticles as drug delivery devices. J Control Release 70:1–20
10. Trapania A, Sitterbergb J, Bakowskyb U, Kissel T (2009) The potential of glycol chitosan nanoparticles as carrier for low water soluble drugs. Int J Pharm 375:97–106
11. Desirée TO, Carmen RL, Alonso MJ (2009) Chitosan/cyclodextrin nanoparticles can efficiently transfect the airway epithelium in vitro. Eur J Pharm Biopharm 71:257–263
12. Trapani A, Lopedota A, Franco M, Cioffi N, Ieva E, Marcos GF, Alonso MJ (2010) A comparative study of chitosan and chitosan/cyclodextrin nanoparticles as potential carriers for the oral delivery of small peptides. Eur J Pharm Biopharm 75:26–32
13. Zhang YF, Yin P, Zhao XQ, Wang J, Wang J, Wang CD, Ren L, Zhang QQ (2009) O-Carboxymethyl-chitosan/organosilica hybrid nanoparticles as non-viral vectors for gene delivery. Mater Sci Eng C 29:2045–2049
14. Dev A, Mohan JC, Sreeja V, Tamura H, Patzke GR, Hussain F, Weyeneth S, Naira SV, Jayakumar R (2010) Novel carboxymethyl chitin nanoparticles for cancer drug delivery applications. Carbohydr Polym 79:1073–1079
15. Cai ZS, Song ZB, Shang SB, Yang CS (2007) Study on the flocculating properties of quaternized carboxymethyl chitosan. Polym Bull 59:655–665
16. Sun LP, Du YM, Fan LH, Chen X, Yang JH (2006) Preparation, characterization and antimicrobial activity of quaternized carboxymethyl chitosan and application as pulp-cap. Polymer 47:1796–1804
17. Lamkin S, Fraiz A (2009) An acid/base disturbance from ibuprofen toxicity. J Emerg Nurs 35:584–585
18. He JX, Wang Y, Cui SZ, Gao YY, Wang SY (2010) Structure and properties of silk fibroin/carboxymethyl chitosan blend films. Polym Bull 59:395–409
19. Lamprecht A, Saumet JL, Roux J, Benoit JP (2004) Lipid nanocarriers as drug delivery system for ibuprofen in pain treatment. Int J Pharm 278:407–414
20. Higuchi T, Connors KA (1965) Phase-solubility techniques. Adv Anal Chem Instrum 4:117–212
21. Williams RO, Mahaguna V, Sriwongjanya M (1998) Characterization of an inclusion complex of cholesterol and hydroxypropyl-b-cyclodextrin. Eur J Pharm Biopharm 46:355–360
22. Stella VJ, Rao VM, Zannou EA, Zia V (1999) Mechanisms of drug release from cyclodextrin complexes. Adv Drug Deliver Res 36:3–16
23. Araujo MVG, Vieira EKB, Lazaro GS, Conegero LS, Ferreria OP, Almeida LE, Barreto LS, Cost NBa, Gimenez IF (2007) Inclusion complexes of pyrimethamine in 2-hydroxypropyl-b-cyclodextrin: characterization, phase solubility and molecular modelling. Bioorgan Med Chem 15:5752–5759
24. Anitha A, Rani VVD, Krishna R, Sreeja V, Selvamurugan N, Nair SV, Tamura H, Jayakumar R (2009) Synthesis, characterization, cytotoxicity and antibacterial studies of chitosan, O-carboxymethyl and N,O-carboxymethyl chitosan nanoparticles. Carbohydr Polym 78:672–677
25. Sun SL, Wang AQ (2006) Adsorption kinetics of Cu (II) ions using N, O-carboxymethyl-chitosan. J Hazard Mater 131:103–111

26. Yoksana R, Jirawutthiwongchai J, Arpo K (2010) Encapsulation of ascorbyl palmitate in chitosan nanoparticles by oil-in-water emulsion and ionic gelation processes. Colloid Surf B 76:292–297
27. Rokhade AP, Agnihotri SA, Patil SA, Mallikarjuna NN, Kulkarni PV, Aminabhavi TM (2006) Semi-interpenetrating polymer network microspheres of gelatin and sodium carboxymethyl cellulose for controlled release of ketorolac tromethamine. Carbohydr Polym 65:243–252
28. Mundargi RC, Shelke NB, Aminabhavi TM (2008) Formulation and in vitro evaluation of novel starch-based tableted microspheres for controlled release of ampicillin. Carbohydr Polym 71:42–53